

Systematic uncertainties in the determination of the primordial ^4He abundance

D. Sauer and K. Jedamzik

Max-Planck-Institut für Astrophysik, Karl-Schwarzschild-Str. 1, 85741 Garching, Germany

Received / Accepted

Abstract. The primordial helium abundance Y_p is commonly inferred from abundance determinations in low-metallicity extragalactic H II-regions. Such determinations may be subject to systematic uncertainties that are investigated here. Particular attention is paid to two effects: *icf*-corrections for “imperfect” ionization structure leading to significant amounts of (unobservable) neutral helium or hydrogen and *tcf*-corrections due to non-uniform temperature. Model H II-regions with a large number of parameters are constructed and it is shown that required corrections are almost exclusively functions of two physical parameters: the number of helium-to hydrogen- ionizing photons in the illuminating continuum $Q(\text{He}^0)/Q(\text{H}^0)$, and the ratio of width to radius $\delta r_S/r_S$ of the Strömgen sphere. For clouds of sufficient helium-ionizing photons $Q(\text{He}^0)/Q(\text{H}^0) \gtrsim 0.15$ and non-negligible width of the Strömgen sphere a significant overestimate of helium abundances may result. Such clouds show radiation softness parameters in the range $-0.4 \lesssim \log \eta \lesssim 0.3$ coincident with the range of η in observed H II-regions. Existing data of H II-regions indeed seem to display a correlation which is consistent with a typical $\sim 2 - 4\%$ overestimate of helium abundances due to these effects. In case such an interpretation prevails, and in the absence of other compensating effects, a significant downward revision of Y_p may result. It is argued that caution should be exercised regarding the validity of commonly quoted error bars on Y_p .

Key words. Cosmology: early Universe – ISM: H II-regions, abundances

1. Introduction

The observational determination of the primordial light element abundances provides an important key test for the validity of the standard model of Big Bang nucleosynthesis and the cosmic baryon density. Within the last years, a large number of high-quality observations of hydrogen- and helium- emission lines originating from extragalactic giant H II-regions and compact blue galaxies has led to a number of determinations of the primordial helium mass fraction Y_p (e.g. Peimbert & Torres-Peimbert 1974; Kunth & Sargent 1983; Pagel et al. 1992; Izotov et al. 1994, 1997; Olive et al. 1997; Izotov & Thuan 1998; Peimbert et al. 2000). Though quoted statistical errors of these Y_p determinations are often $\lesssim 1\%$ due to the size of the employed samples, it is by now widely accepted that errors in the inferred Y_p may be dominated by systematic uncertainties. Only in this way, may one understand how different groups arrive at either high $Y_p \approx 0.244$ (Izotov & Thuan 1998) or low $Y_p \approx 0.234$ (Olive et al. 1997; Peimbert et al. 2000) values which deviate by several times the quoted statistical error.

It seems presently feasible to determine the primordial D/H ratio to unprecedented accuracy by observations of quasar absorption line systems (Burles et al. 1999; O’Meara et al. 2000; Tytler et al. 2000). These observations favor a “low” primordial deuterium abundance, i.e. $\text{D}/\text{H} \approx 3 \times 10^{-5}$, implying a baryonic contribution to the critical density of $\Omega_b h^2 \approx 0.02$ (with h the Hubble constant in units of $100 \text{ km s}^{-1} \text{ Mpc}^{-1}$), and a primordial helium abundance of $Y_p \approx 0.247$, within the context of a standard Big Bang nucleosynthesis scenario. The accurate observational determination of Y_p would not only give an independent “measurement” of $\Omega_b h^2$, but would also allow for a test of the validity of a standard Big Bang nucleosynthesis scenario. Such an undertaking, nevertheless, would require Y_p determinations with statistical and systematic errors $\lesssim 1\%$, a magnitude which requires investigation of a large number of possible errors which may enter the analysis.

Beyond the pure random errors that generally underlie any measurement, there are several sources of systematic uncertainty in commonly used observational techniques and subsequent analysis of spectra of giant H II-regions for the determination of helium (and metal) abundances. To a first approximation, helium abundances in nebulae can be easily inferred by observing the relative line fluxes of

Send offprint requests to:

D. Sauer, e-mail: dsauer@mpa-garching.mpg.de or

K. Jedamzik, e-mail: jedamzik@mpa-garching.mpg.de

lines produced during helium recombinations (Peimbert & Torres-Peimbert 1974) and lines produced during hydrogen recombinations (e.g. $H\beta$),

$$\frac{I(\text{He I}, \lambda)}{I(H\beta)} = \frac{\int n_e n_{\text{He}^+} \alpha_{\text{He}}^{\text{eff}}(\lambda, T)}{\int n_e n_{\text{H}^+} \alpha_{\text{H}}^{\text{eff}}(H\beta, T)} \propto \frac{\text{He}}{\text{H}} \quad (1)$$

when cloud temperature T and the effective recombination coefficients α_i^{eff} (cf. Osterbrock 1989) are known. The influence of systematic errors starts at the correction for effects of reddening, underlying stellar absorption (i.e. correcting for absorption troughs in the stellar continuum at the position of the emission lines), and fluorescent enhancement of helium lines (e.g., through absorption of He I $\lambda 3889$ by the metastable 2^3S level of He I and re-emission as He I $\lambda 7065$). The use of Eq. (1) also presumes that there is no contribution to the observed line radiation from collisional excitation, an effect which becomes important particularly at higher densities. Izotov & Thuan (1998) have devised a method to correct these potential errors simultaneously by employing several He I emission lines in the analysis. This method (and others) has also been recently critically assessed by Olive & Skillman (2000) (see also Sasselov & Goldwirth 1995), with the result that residual errors may still be appreciable. Uncertainties in the theoretically computed effective recombination coefficients could also introduce systematic errors as large as $\sim 1.5\%$ (Benjamin et al. 1999).

The largest systematic errors, nevertheless, may result from the idealizing assumptions that H II-regions are clouds at constant temperature and density, with simple geometry, and with helium- and hydrogen- Strömgen sphere radii coinciding to within one percent. These assumptions enter implicitly in an analysis which follows the strategy of Eq. (1). In this paper the validity of two of these assumptions are tested in detail: the assumption of constant temperature (the deviation of this case is commonly referred to as the existence of “temperature fluctuations”) and the assumption of equal Strömgen spheres (correction for this effect is commonly achieved by factoring in “ionization correction factors (*icf*)”). The latter (*icf*) effect is usually only considered by estimating the quality of the incident continuum by the “Radiation Softness Parameter” η (Vilchez & Pagel 1988; Skillman 1989) and based on model calculations by Stasińska (1990) it has been assumed that for sufficiently hard radiation ($\log \eta < 0.9$) *icf*-corrections are negligible ($< 1\%$, Pagel et al. (1992)). Nevertheless, the potential importance of ionized helium in regions where hydrogen is almost completely neutral has been recently stressed by a number of groups (Armour et al. 1999; Viegas et al. 2000; Ballantyne et al. 2000). (The problem was already noted earlier e.g. by Stasińska (1980), Dinerstein & Shields (1986), and Peña (1986).) New model calculations therein confirmed the presence of this problem. The present work is distinguished from prior analyses by the consideration of a much larger number of model H II-regions and incident stellar spectra. It also reaches a somewhat different conclusion about the importance of this problem.

Effective recombination coefficients α^{eff} employed to infer ionic abundances from observed emission line ratios are functions of the electron temperature within the emitting volume. Temperatures in H II-regions are usually inferred from flux ratios of collisionally excited oxygen lines (i.e. $[\text{O III}]\lambda\lambda 4959, 5007/4363$) and are mostly approximated to be constant (cf. Peimbert et al. (2000) for an analysis going beyond this). Since collisionally excited lines are exponentially sensitive to temperature, a temperature determination by such methods is systematically biased to the hottest parts of the H II-region. However, those regions which are somewhat colder may contribute most of the helium- and hydrogen recombination lines. A systematically overestimated electron temperature will also lead to an overestimate of Y_P . The problem of the choice of an appropriate mean electron temperature for recombination coefficients was discussed in detail by Peimbert (1967). A discussion of the temperature effect pertaining to the determination of Y_P has also appeared in the work of Steigman et al. (1997), who gauge the effect by somewhat arbitrarily changing inferred temperatures. The present work analyses this problem by constructing models for H II-regions with a photoionization code (CLOUDY 90.05 (Ferland 1997)).

The general strategy of this paper is as follows. The simplest possible, spherically symmetric, H II-regions at constant (and low) density are constructed and their emission spectra are calculated with the help of a photoionization code. These models include a variety of parameters. Degeneracies of the resultant emission spectra to these parameters are outlined. Ranges of typical emission line ratios are inferred from observed H II-regions, and a model H II-region is accepted only if it falls into these ranges. Correction factors *icf* and *tcf* are defined which quantify the appropriate ionization correction and correction for temperature inhomogeneity needed to infer the “true” helium abundance. These factors equal unity for the ideal ionized, “one zone” cloud. Finally, the obtained *icf* and *tcf* correction factors will be compared to observational diagnostic tools (i.e. Radiation Softness Parameter and $[\text{O III}]\lambda 5007/[\text{O I}]\lambda 6300$ ratios) as well as to the H II-region sample by Izotov & Thuan (1998).

In Sect. 2 the model calculations and the parameters employed in the calculations are described. Detailed results for the required ionization correction and temperature correction factors are presented in Sect. 3 and discussed more broadly in Sect. 4. Conclusions are drawn in Sect. 5.

2. Models of H II-Regions

The model H II-regions are calculated using the photoionization code CLOUDY Version 90.05 (Ferland 1997). In all models a spherical symmetric distribution of gas around a compact, point-like source of ionizing radiation at the center is assumed. All models have a constant (total) hydrogen number density of $n_{\text{H}} = 10 \text{ cm}^{-3}$. This relatively small density is chosen to ensure that collisional enhancement

of helium recombination lines is negligible. Further, it is assumed that effects of radiative transfer can be treated in the On-The-Spot approximation. Thus the emission of recombination lines may be described using the well-known Case B limit. Note that the photoionization code Cloudy has been slightly modified to employ helium emissivities relative to $H\beta$ as given in Pagel et al. (1992). In the limit of small density these are practically identical to those given in Benjamin et al. (1999). The model clouds investigated here are ionization bounded, i.e. the edge of the cloud is defined by the Strömgen sphere where the degree of ionization of hydrogen drops rapidly to zero. In this case all UV-photons with $h\nu > 13.6$ eV are absorbed and eventually converted into lower energy photons.

The adopted abundances of heavy elements are those given by Bresolin et al. (1999). These are based on the compilation by Grevesse & Anders (1989), but with depletion on dust grains taken into account. In order to simulate H II-regions with metallicities far below solar, all elements heavier than helium are scaled down in abundance by the same factor. The employed metallicities in the model calculations range between $Z/Z_\odot = 1/36$ and $1/12$, corresponding to $10^6 O/H = 23.64$ to 70.93 . The effects of dust grains, themselves, on, for example, the reddening of lines or the heating/cooling balance, is not specifically considered. Assuming that the density of dust scales with metallicity, these effects should be fairly small for the clouds considered. The helium abundance was kept constant for all models at a value of $He/H = 0.0776$.

Given the hydrogen number density n_H , the spectrum of the ionizing background, and the metallicity of the cloud, there are three remaining parameters describing the simulated H II-regions. These are $Q(H)$ the number of photons with $h\nu > 13.6$ eV radiated by the source in unit time, r_0 the inner radius of the cloud, and ϵ the volume filling factor of gas at density n_H taking into account the effect of gas condensations in H II-regions (see e.g. Osterbrock & Flather 1959). Nevertheless, it will be shown that the variation of only one of these parameters ($Q(H)$, r_0 , or ϵ) is necessary to generate H II-regions with different emission spectra. The quantities $Q(H)$, n_H , ϵ , and r_0 define the ionization parameter U_S , i.e. the approximate number of ionizing photons per hydrogen at the hydrogen Strömgen sphere r_S :

$$U_S = \frac{Q(H)}{4\pi r_S^2 n_H c}. \quad (2)$$

Here the Strömgen sphere radius r_S may be somewhat arbitrarily defined as the location where $n_{H^0}/n_{H^+} = 1$. The parameter U_S fully determines the structure of a spherically symmetric cloud for a given chemical composition and incident continuum. Thus clouds with the same U_S , but different n_H , $Q(H)$, and ϵ are self-similar in their ionization structures. Except for the total luminosity, such self-similar clouds will result in the emission of essentially identical nebular spectra. This assumes that the effects of collisional excitation on the heating/cooling balance and the line emission are negligible. This is typically applicable

for densities $n_H \ll 100\text{cm}^{-3}$. Moreover, as long as models have $r_S \gg r_0$, the exact choice of the parameter r_0 is of secondary importance for the calculation of nebular emission spectra. This is primarily because the regions in the very interior of the cloud contribute very little to the total line emission due to the small amount of gas involved. When $r_S \gg r_0$ one can show from the balance of hydrogen ionizations to recombinations that U_S is proportional to

$$U_S \propto (Q\epsilon^2 n_H)^{1/3}. \quad (3)$$

Note that this definition of the ionization parameter leads to an increase of U_S with increasing n_H in contrast to the ionization parameter at the inner radius of the cloud $U_0 = n_\gamma/n_H(r_0)$, which is often used as the input parameter to specify the relative photon to gas density in plane-parallel clouds. Figure 1 illustrates this proportionality Eq. (3) of U_S for a sample of models with varying $Q(H)$, r_0 , and ϵ . The few models that do not satisfy Eq. (3) are those where $r_S \sim r_0$, in particular, where shell geometry pertains. In what follows, it is therefore not necessary to vary $Q(H)$, r_0 , and ϵ independently, but rather analyze clouds with different U_S , the physical parameter determining the emission spectra when the geometry of the H II-regions is characterized by a sphere.

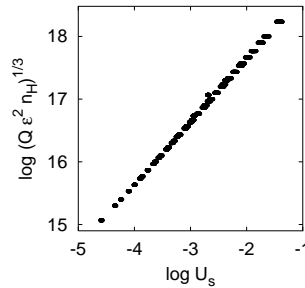


Fig. 1. Relationship between Q , ϵ , and U_S for a sample of models ionized by a Mihalas (1972) continuum with $T_{\text{eff}} = 45\,000$ K. The few models that are more distant from the line of proportionality are those where the assumption of a solid sphere with $r_0 \ll r_S$ is no longer valid (see text).

Incident Continuum: The effects studied here are particularly sensitive to the shape of the incident continuum at energies higher than 1 Ryd. Spectra with a larger contribution of helium ionizing photons cause an ionization structure where the Strömgen sphere of helium is equal or even larger than the Strömgen sphere of hydrogen. These are spectra of O and early B stars with effective temperatures above $T_{\text{eff}} \sim 40\,000$ K. The effective temperature of an entire star cluster has these high values during the early stages of its evolution. In this case the spectrum is dominated by the most massive and, thus, hottest stars. Since massive stars burn out more quickly than less massive ones, at later times, the main contribution to the ionizing spectrum is increasingly provided by cooler stars. This, in turn, implies a radiation spectrum of the cluster which is softer. In this paper several different spectra for the ionizing radiation are used. These include two different spectra for single stars at various effective temperatures, in particular, spectra computed from the non-LTE plane-parallel

stellar atmospheres by Mihalas (1972) and the LTE plane-parallel atmospheric grids by Kurucz (1991). These continua are shown in Figure 2 for one effective temperature. For reference, a blackbody spectrum of the same temperature is also shown in the diagram. All plotted spectra are normalized to have the same number of ionizing photons. From left to right, the vertical lines indicate the threshold energies for ionization of H^0 , He^0 , and He^+ , respectively.

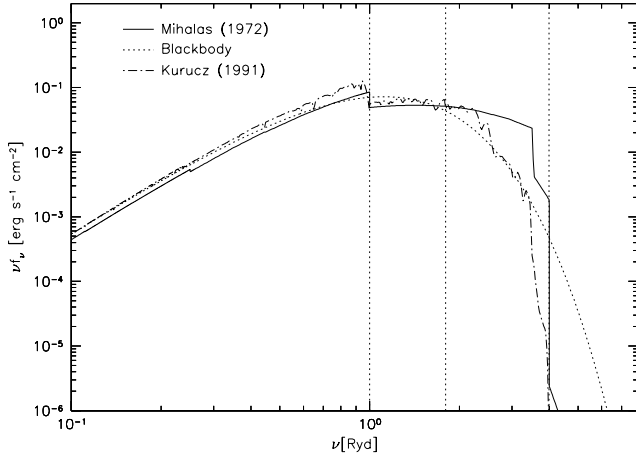


Fig. 2. Single star spectra by Mihalas (1972) and Kurucz (1991). Both are shown for an effective stellar temperature $T_{\text{eff}} = 45\,000\text{ K}$ and for the same number of hydrogen ionizing photons $Q(H) = 10^{51}\text{ s}^{-1}$. For comparison, a blackbody spectrum with the same parameters is shown as well. Fluxes are given at a distance of 73 pc to the star. From left to right, the vertical lines show the threshold energies for ionization of H^0 , He^0 and He^+ .

In addition, this work also employs spectra appropriate to a whole cluster of stars. These starburst spectra were generated by using the starburst synthesis code STARBURST 99 (Leitherer et al. 1999). The synthesis was performed by adopting instantaneous star formation with Salpeter IMF exponent 2.35. The population of stars had an upper mass limit of $150M_{\odot}$ and a fixed stellar mass of $8.7 \times 10^4 M_{\odot}$. The evolution of the stellar cluster was described by the standard mass loss tracks with metallicity $Z = 0.001$ (i.e. $Z/Z_{\odot} = 1/20$). The stellar atmospheres needed to calculate spectra were those from Kurucz (1992) and Schmutz et al. (1992). A sample of spectra with different ages is shown in Figure 3. One may see that for longer cluster ages, the main contribution to the spectrum originates from cooler stars and the spectrum becomes softer. Note that in addition to the above mentioned spectra we have also performed test calculations with Costar stellar spectra Schaerer & de Koter (1997) as well as with spectra given by Pauldrach et al. (1998). In what follows results for these spectra, which show generally the same trends as those considered in detail, are not shown.

One parameter characterizing the “hardness” of the incident continuum is the ratio of the number of helium

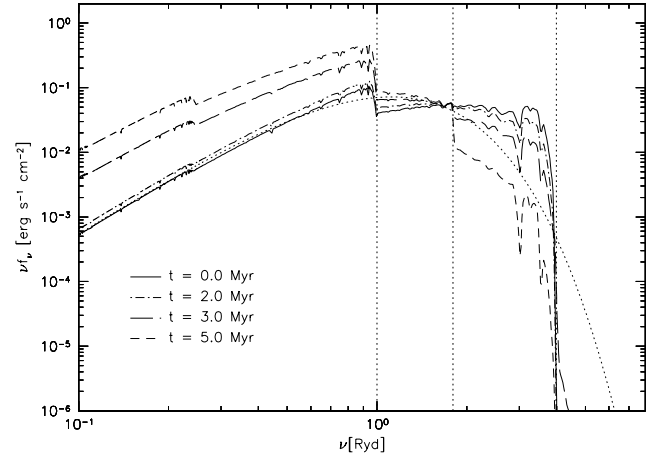


Fig. 3. The continua emitted by stellar clusters of different ages with metallicity $Z/Z_{\odot} = 1/20$ (see text for details). The dotted line shows a blackbody emission with the same effective temperature while the vertical dotted lines indicate the ionization frequencies of H^0 , He^0 and He^+ .

ionizing photons ($h\nu > 1.8\text{ Ryd}$) to that of hydrogen ionizing photons ($h\nu > 1\text{ Ryd}$), i.e. $Q(He^0)/Q(H^0)$. (In addition, the number of He^+ ionizing photons can be taken into account, although in case of the spectra used here, this contribution is small.) Figure 4 shows this ratio for the spectra employed in this work. The total luminosity of the incident continuum is set by specifying the total number of hydrogen ionizing photons $Q(H)$ emitted by the source into 4π .

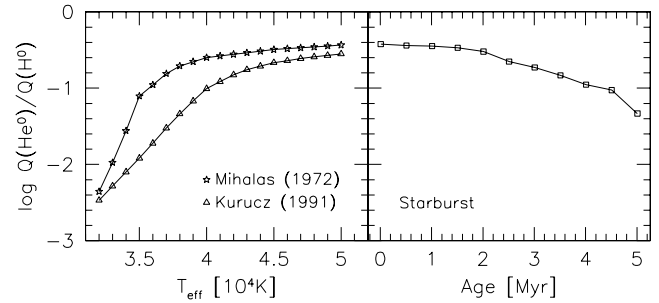


Fig. 4. Ratio of the number of helium ionizing photons to hydrogen ionizing photons as emitted by different stellar continuum sources. The left panel shows the single star spectra by Mihalas (1972) and Kurucz (1991), whereas the right panel refers to continua of a stellar cluster calculated with STARBURST99 (Leitherer et al. 1999) for metallicity $Z/Z_{\odot} = 1/20$

Constraints from Observations: In this work, it is not intended to exactly model one specific cloud, but rather,

to simulate the whole class of low-metallicity H II-regions which is employed to infer helium abundances. Whether or not a model is suitable to describe the structure and emission of H II-regions used for ^4He determination may be decided by verifying if the physical parameters adopted for the H II-regions lead to numerically calculated spectra which resemble those of the observations. Therefore, one may choose “realistic” models according to whether their emission characteristics fall broadly within certain observationally acceptable ranges. As a guideline for typical line emission observed in clouds that are employed for primordial helium abundance determinations, the sample from Izotov et al. (1997) has been used. Particular importance is placed to those emission features which are used to infer main properties of the cloud as well as helium abundances. Ranges for these lines are defined from the observational sample. They cover the emission characteristics of the whole sample in these specific lines. Table 1 shows these ranges that the emission line ratios of a “realistic” model have to be within.

In Figure 5, each panel shows a grid of models of different metallicity, where the parameters luminosity $Q(\text{H})$ and filling factor ϵ are varied, respectively. The filled dots indicate those models, where the relative emission line intensities are within the ranges given in Table 1, while the remaining models are shown by open circles. It is evident that the acceptable models display a band structure. Models along these bands are self-similar, with essentially identical emission spectra but varying total luminosity, in particular, they are described by the same U_S (cf. Eq. 2). In the orthogonal direction (from the lower left towards the upper right corner) the ionization parameter U_S increases. The same applies for the temperature within the cloud. Thus, below the band of suitable models, the line ratios of temperature sensitive emission lines like the forbidden metal lines, tend to lower values than observed; whereas, models above the band show emission that is too strong in these lines. Towards higher metallicity, more models with smaller U_S fulfill the range criterion. The emission from lower ionization stages of heavy element ions indicates the significance of ionization fronts at the outer boundaries of the cloud. These regions become more important relative to the main body for lower U_S , as will be explained below.

3. Results of the Model Calculations

3.1. Ionization Structure

The determination of helium abundances in H II-regions possibly requires a correction for unseen ionization stages of hydrogen or helium. When the stars ionizing the nebulae are not too hot (late O stars and later), the supply of helium-ionizing photons might not be sufficient to maintain a high fraction of He^+ throughout the whole hydrogen Strömgren sphere. Vice versa, for hard spectra of the ionizing source it is also possible that a helium Strömgren sphere larger than the one of hydrogen is set up (Stasińska

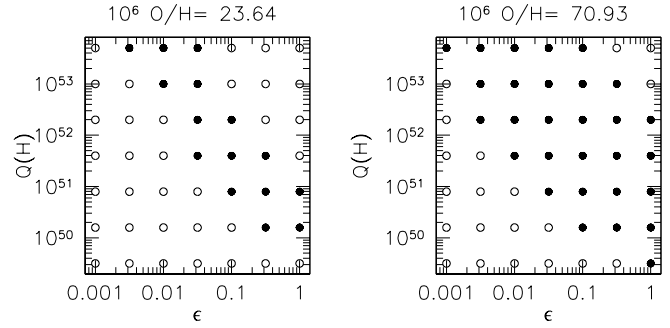


Fig. 5. The luminosity $Q(\text{H})$ – filling factor ϵ parameter space of “acceptable” models for two different metallicities, as labeled. Filled squares indicate the models that fulfill the range criterion (see Table 1) while open circles are those where one or more lines are not within the observed ranges. All models in this figure were calculated using the Mihalas (1972) spectrum with $T_{\text{eff}} = 45\,000\text{ K}$. For other spectra, the structure of the diagram stays similar. The parameter U_S stays constant along this band structure.

Ion	$\lambda [\text{\AA}]$	$I(\lambda)/I(\text{H}\beta)$	
		min	max
[O II].....	3727	0.170	4.400
Ne [III]....	3869	0.130	0.890
He I.....	3889	0.010	0.300
Ne [III]+H7	3968	0.000	0.500
H δ	4101	0.220	0.320
H γ	4340	0.410	0.620
[O III]....	4363	0.030	0.195
He I.....	4471	0.010	0.060
He II.....	4686	0.000	0.035
[O III]....	4959	0.500	2.500
[O III]....	5007	1.500	9.200
He I.....	5876	0.007	0.130
[O I].....	6300	0.000	0.500
[S III]....	6312	0.000	0.037
H α	6563	2.540	3.100
He I.....	6678	0.007	0.050
[S II].....	6717	0.019	0.500
[S II].....	6731	0.014	0.374
He I.....	7065	0.010	0.040

Table 1. Range criteria for the line emission in wavelength λ to be fulfilled by the model H II-regions. Fluxes I are given relative to $\text{H}\beta$. The intervals refer to the values that are observed by Izotov et al. (1997). Some limits are relaxed by 3-10% to take into account possible deviations of real clouds from the idealized assumptions of the model calculations.

1980; Dinerstein & Shields 1986; Peña 1986; Armour et al. 1999; Viegas et al. 2000; Ballantyne et al. 2000). Recently, it has been attempted to correct for this effect, i.e. the existence of neutral hydrogen (Viegas et al. 2000; Ballantyne et al. 2000), though these studies reach opposite conclu-

sions about the induced systematic uncertainty on the inferred $Y_{\mathcal{P}}$.

Another possible systematic error due to the ionization structure of H II-regions arises from the fact that the observed emission lines are always weighted towards regions with higher electron density. The intensity in a particular He I recombination line relative to a reference line like H β is given by

$$\frac{I(\text{He I}, \lambda)}{I(\text{H}\beta)} = \frac{\int n_e n_{\text{He}^+} \alpha_{\text{He}}(\lambda, T) dV}{\int n_e n_{\text{H}^+} \alpha_{\text{H}}(\text{H}\beta, T) dV} \quad (4)$$

Here n_e is the electron number density, n_{He^+} and n_{H^+} are the number densities of He^+ and H^+ , respectively, and $\alpha_i(\lambda, T)$ are the recombination coefficients of the lines λ considered as a function of electron temperature T . Thus, in regions where the electron density is small, the emission of a line becomes weaker even if the density of the emitting ion itself stays constant. If n_e is not constant within the whole volume, though, the intensity ratio in Eq. (4) is not proportional to He^+/H^+ even when the electron temperature and, thus recombination coefficients α , stay constant over the cloud volume. This effect becomes particularly important for clouds where the Strömgren sphere of hydrogen is smaller than the one for helium. This is due to the small abundances of all other elements, in particular, H^+ provides the main contribution to n_e . But also in case of a He^+ sphere smaller than the H^+ sphere this effect needs to be considered. The coupling of the ionization equilibrium equations of helium and hydrogen for photons with $h\nu \geq 24.6$ eV, causes variations in n_e resulting in smaller He I recombination line emission (Sasselov & Goldwirth 1995).

In order to correct the observationally inferred helium abundances for unseen ionization stages, usually an ‘‘ionization correction factor’’ icf is introduced. The significance of this effect, is then estimated by comparing certain emission lines that provide information on the incident continuum and, in turn, on the ionization structure. In contrast to the definition of icf that is used by Viegas et al. (2000), Armour et al. (1999) and others, icf^* as it is introduced here, corrects for both, unseen helium ionization stages He^0 and He^{2+} , and the effect arising from varying electron density within the observed volume (see Stasińska 1990). The definition of the ionization correction factor by Stasińska (1980), that is employed in the work of Pagel et al. (1992) and Izotov et al. (1994, and subsequent papers), takes the electron density into account. However, in these works icf^* is assumed to be unity in most cases. (See the discussion later.) In the present work icf^* is defined as the ratio of the true helium abundance relative to hydrogen and the amount of ionic helium to hydrogen within the volume V that is emitting line radiation at all:

$$icf^* = \left(\frac{\int n_{\text{He}} dV}{\int n_{\text{H}} dV} \right) \left/ \left(\frac{\int n_{\text{He}^+} dV}{\int n_{\text{H}^+} dV} \right) \right. \times \left. \left(\frac{\int n_{\text{He}^+} dV}{\int n_{\text{H}^+} dV} \right) \left/ \left(\frac{\int n_e n_{\text{He}^+} dV}{\int n_e n_{\text{H}^+} dV} \right) \right.$$

$$= \frac{\int n_{\text{He}} dV}{\int n_{\text{H}} dV} \left/ \frac{\int n_e n_{\text{He}^+} dV}{\int n_e n_{\text{H}^+} dV} \right. \quad (5)$$

Note that the inclusion of correction for He^{2+} in Eq. (5) may be omitted, as the abundance of this ion may be observationally inferred from $\lambda 4686$ line radiation. In the models used here the abundance of doubly ionized helium is essentially negligible, such that both definitions would coincide. The first factor in the first equation of Eq. (5) may be identified as the ionization correction for constant electron density. It is important to realize that the effect of varying electron density, taken into account by the second factor in this equation, implies a required correction which, in almost all cases, is significantly smaller (i.e. $|(icf^* - 1)/(icf - 1)| < 1$) than the one where the effect is omitted.

3.1.1. General Trends:

In the following, general trends of the required ionization correction factors for clouds with varying parameter U_S and for ionizing sources of different spectra are studied. Figure 6 shows the relation between U_S and icf^* for the whole sample of models. The models that fulfill the range criterion discussed above, are shown as black filled symbols. Each track in this figure corresponds to a grid of models ionized by the same continuum. The lower tracks result from relatively hard spectra (i.e. high T_{eff}) while for softer spectra icf^* tends towards larger values. (Continua were chosen in steps of 1000 K or 0.5 Myr, respectively.) Furthermore, it may be seen that when the spectrum of the ionizing source is fixed icf -corrections generally become more pronounced for smaller ionization parameter U_S . It is evident from the figure that systematic errors in-

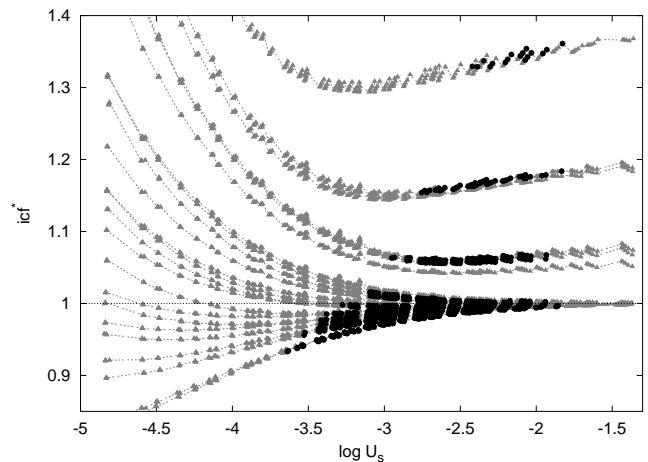


Fig. 6. Ionization correction factors as a function of ionization parameter at the Strömgren sphere U_S . Dark symbols refer to models fulfilling the range criteria. All models employed in this work are shown.

duced by the ionization structure may, in principle, grow

quite large. Even for models, that show emission line characteristics similar to those observed in H II-regions employed for ${}^4\text{He}$ determinations (black symbols) this potential error ranges from an overestimate of ${}^4\text{He}$ by up to $\sim 7\%$ to an underestimate by up to $\gtrsim 30\%$. It will be shown below, however, that existing observational data on low-metallicity H II-regions seems consistent with a possible ${}^4\text{He}$ overestimate, rather than a ${}^4\text{He}$ underestimate.

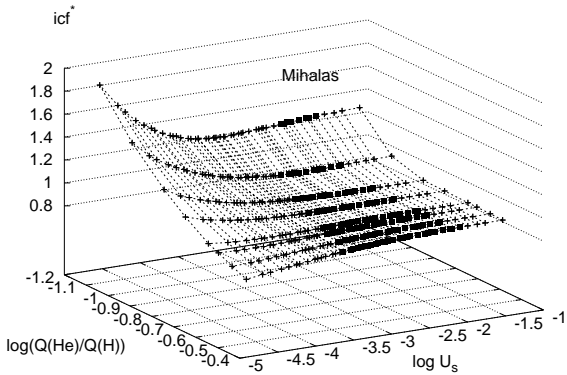


Fig. 7. icf^* versus $Q(\text{He}^0)/Q(\text{H}^0)$ and U_S for clouds ionized by Mihalas (1972) spectra. Dark squares refer to models fulfilling the emission line range criterion.

Influence of the Incident Continuum: To study the influence of the incident continuum on the ionization corrections in more detail, subsamples were analyzed. Fig. 7 shows the derived icf^* of models ionized by different spectra as a function of the $Q(\text{He}^0)/Q(\text{H}^0)$ -ratio and the ionization parameter U_S . Though the particular figure employs Mihalas spectra for the ionizing radiation, the general trends of the figure are hardly changed when other ionizing spectra are employed. This is mainly due to the choice of more physical $Q(\text{He}^0)/Q(\text{H}^0)$ -ratios as characteristics of the spectra, rather than the effective stellar temperatures. It may be seen that for clouds ionized by relatively soft spectra (small values of $Q(\text{He}^0)/Q(\text{H}^0)$) the icf^* is larger than unity for all U_S . When the hardness of the spectrum is increased, the icf^* correction approaches unity until a critical value for $Q(\text{He}^0)/Q(\text{H}^0)$ is reached. For values larger than about $Q(\text{He}^0)/Q(\text{H}^0) \gtrsim 0.15$ required ionization corrections reverse such that values of icf^* smaller than unity obtain. This trend is observed to be more dramatic for smaller U_S , where the icf^* may deviate significantly from unity. From an observational point of view it would be desirable to infer helium abundances within clouds with $U_S \gtrsim 10^{-2}$ and $Q(\text{He}^0)/Q(\text{H}^0) \gtrsim 0.2$ where at least within the simple models analyzed here icf -corrections are within a per cent.

Qualitatively, these trends may be understood as follows: For soft spectra the supply of He ionizing UV-photons emitted from the central source is not sufficient to ionize He throughout the H^+ sphere regardless of the ionization parameter. This leads to $icf^* > 1$. Only photons with $h\nu \geq 24.6 \text{ eV}$ may ionize helium, whereas all photons with $h\nu \geq 13.6 \text{ eV}$ may ionize hydrogen. In the “best” case scenario (for maximum helium ionization of a radiation bounded nebula) all $h\nu \geq 24.6 \text{ eV}$ will be absorbed by helium such that the ionization equilibria of hydrogen and helium may be treated separately. Then for $icf^* > 1$ the relation

$$icf^* \propto \frac{n_{\text{He}}}{n_{\text{H}}} \left(\frac{Q(\text{He}^0)}{Q(\text{H}^0)} \right)^{-1} \quad (6)$$

approximately holds. This expression neglects the emission of hydrogen ionizing radiation during helium recombination, as well as assuming $Q(\text{He}^0) \ll Q(\text{H}^0)$. It, nevertheless, clarifies the existence of a critical $Q(\text{He}^0)/Q(\text{H}^0)$ where icf^* tends towards corrections larger than unity, irrespective of U_S . This critical value depends on the helium content relative to hydrogen.

There exists an additional effect which leads to icf^* deviating from unity, even when there is a sufficient supply of helium ionizing photons. For decreasing U_S , the width of the Strömgen sphere δr_S increases relative to the Strömgen radius r_S . The width δr_S is given by the distance over which ionizing radiation in partially neutral gas has optical depth of order unity, i.e. $\tau \approx \sigma_{ph} \epsilon n_{\text{H}} \delta r_S \approx 1$. Here σ_{ph} is an appropriate photoionization cross section. From this one may show that $\delta r_S/r_S$ relates to U_S via

$$\delta r_S/r_S \approx 5 \times 10^{-7} U_S^{-1} \quad (7)$$

as long as $r_S \gg r_0$, and under the assumption of constant density across the ionization front. Since the relative volume of gas in the transition region to that in the essentially completely ionized body of the cloud is $\sim 3\delta r_S/r_S$ the effects of emission from partially ionized gas become increasingly important for small U_S . This implies significant ionization corrections for small U_S , overestimating helium abundances for $Q(\text{He}^0)/Q(\text{H}^0) \gtrsim 0.15$ and underestimating helium abundances in the opposite case. Thus icf effects become asymptotically unimportant only for spectra that have sufficient emission of helium ionizing photons and for Strömgen sphere ionization parameters which are sufficiently large.

3.1.2. Observational Tools

Because neither the ionization parameter U_S itself nor the ratios of different Q -values are directly observable, other quantities have to be found in order to estimate the influence of ionization structure on the inferred abundances.

Radiation Softness Parameter: One frequently chosen method compares the abundance ratios O^+/O^{++} and S^+/S^{++} . This provides a measure for the quality of the

incident spectrum with respect to its ionizing ability. This “Radiation Softness Parameter”

$$\eta = \frac{O^+ S^{++}}{S^+ O^{++}}, \quad (8)$$

originally introduced by Vilchez & Pagel (1988), is often used to “read off” the ionization correction from model calculations like those performed by Stasińska (1990). Usually, first the particular ionic abundances are inferred from their respective emission lines, then η is derived from these results following the definition of Eq. (8). Here the particular choice of emission lines employed for the ionic abundance determinations may differ slightly between different authors (see e.g. Pagel et al. 1992). In many observational determinations of helium abundances, the ionization correction for He is simply assumed to be negligible for H II-regions that are ionized by sufficiently hard spectra leading to small values of η . For instance, Pagel et al. (1992) adopt no correction (i.e. $icf^* \equiv 1$) for those nebulae where $\log \eta < 0.9$ and exclude objects with larger η from their analysis. Izotov & Thuan (1998), more or less, follow this procedure. Corrections < 1 are usually not considered. The $\log \eta$ of the objects which this group uses for helium determinations, are all within the interval of $-0.2 < \log \eta < 0.4$. Figure 8 shows the values for η as a function of the ionization parameter U_S and the ratio $Q(\text{He}^0)/Q(\text{H}^0)$. From this figure it is evident that $\log \eta$ has not only a dependence on the quality of the spectrum, as often assumed, but also on the parameter U_S . H II-regions which would be ideally suitable for helium abundance determinations would have extremely low $\log \eta < -0.5$, since, following the discussion from above, they would have large U_S and $Q(\text{He}^0)/Q(\text{H}^0)$ above the critical value. Unfortunately, such regions seem not to be easily found in observational surveys. Note here that clouds illuminated by Kurucz (1991) spectra typically show larger $\log \eta$ for the same $Q(\text{He}^0)/Q(\text{H}^0)$ and U_S than those illuminated by either Mihalas (1972) or STARBURST 99 spectra. This shift is mainly caused by the generally much smaller emission of photons that ionize O^+ ($h\nu = 2.58 \text{ Ryd}$) in Kurucz (1991) spectra.

Figure 9 shows the calculated icf^* versus the Radiation Softness Parameter η . The η of the H II-regions from the sample of Izotov et al. (1997) are within the interval that is indicated in this figure by the two vertical lines. The figure shows, that icf^* may become significantly smaller than unity leading to a potential overestimate of the helium abundance in these clouds of up to $\sim 6\%$ if no correction is applied.

Oxygen-line cutoff-criterion: More recently Ballantyne et al. (2000) suggested two interesting criteria possibly suitable for an estimate of the significance of ionization corrections. The first one involves the $[\text{O III}]\lambda 5007$ line relative to $\text{H}\beta$ and, thus, depends on the metallicity. The

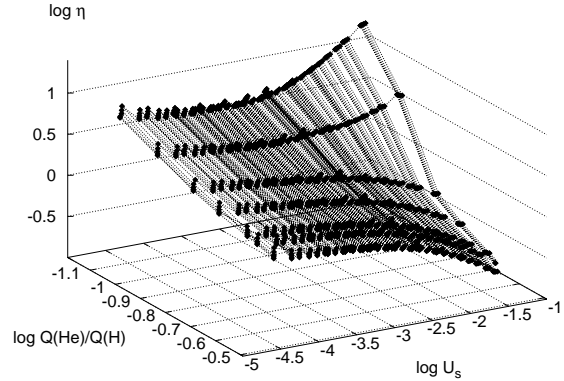


Fig. 8. Dependency of the Radiation Softness Parameter η on the ionizing photon $Q(\text{He}^0)/Q(\text{H}^0)$ ratio and the ionization parameter U_S . This figure shows a sample of models ionized by Mihalas (1972) continua of different effective temperatures.

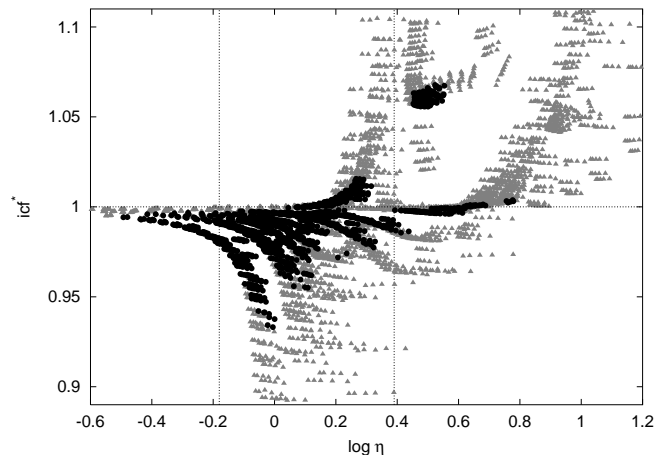


Fig. 9. Derived values of icf^* versus the Radiation Softness Parameter η . The vertical lines indicate the range of η values of the sample investigated in Izotov et al. (1997).

second criterion employs the ratio $[\text{O III}]\lambda 5007/[\text{O I}]\lambda 6300$ and should be approximately independent of metallicity:

$$\left(\frac{[\text{O III}]\lambda 5007}{[\text{O I}]\lambda 6300} \right)_{\text{cutoff}} = 300 \quad (9)$$

and

$$\left(\frac{[\text{O III}]\lambda 5007}{\text{H}\beta} \right)_{\text{cutoff}} = (0.025 \pm 0.004) \left(\frac{\text{O}}{\text{H}} \right) \times 10^6 + (1.39 \pm 0.306) \quad (10)$$

They state that all objects observed with emission ratios lower than these cutoff values should be excluded from consideration since they may be subject to large “reverse”

ionization corrections. Figures 10 to 12 show the results of our calculations in terms of these criteria. It may be seen that the potential error due to $icf < 1$ at the cutoff is still significant and may reach values up to 5%. From these results it is obvious, that the suggested cutoffs are still too optimistic and even larger values have to be employed. Unfortunately, there is a scarcity of observed H II-regions which have sufficiently large $\lambda 5007/\lambda 6300$ or $\lambda 5007/H\beta$ to reduce icf -corrections to a small magnitude. The main difference between our models and the models calculated by Ballantyne et al. (2000) is the geometry. The icf corrections tend towards larger values in spherical geometry as the outer regions of the cloud where preferably lower degrees of ionization are found, contribute more to the total emission in a particular line than in the plane parallel case. Nevertheless, our disagreement with the paper of Ballantyne et al. (2000) on the required cutoff values for negligible icf -correction is not due to geometry. Rather, the proposed cutoffs by Ballantyne et al. (2000) are not sufficient to exclude potentially large reverse icf effects (Ferland 2000).

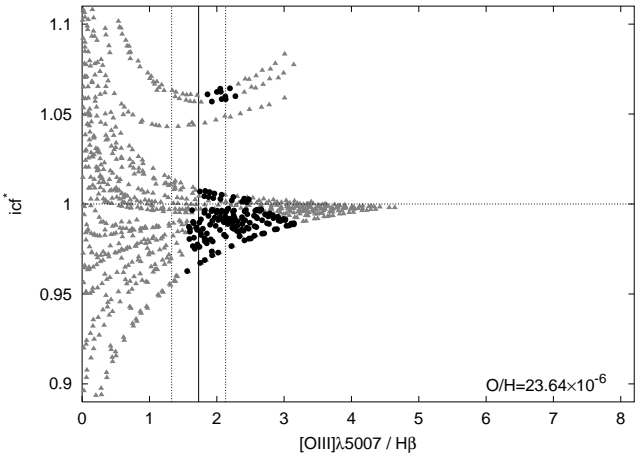


Fig. 10. Metallicity dependent cutoff criterion suggested by Ballantyne et al. (2000). Shown are the derived values for icf^* versus the emission of $[O III]\lambda 5007$ relative to $H\beta$ for models with low metallicity. The vertical lines indicate the suggested cutoff and its error.

3.2. Temperature Variations

In a second focus of this paper, uncertainties are investigated that may occur from the commonly used technique to obtain a suitable electron temperature T_e for helium and hydrogen recombination coefficients. Even in homogeneous, constant density model nebulae, the temperature shows variations (i.e. a temperature stratification), whereas the abundance estimates employing emission lines usually assume a constant temperature. Following prior literature we sometimes refer to this temperature stratification as the existence of temperature ‘fluctuations’. The

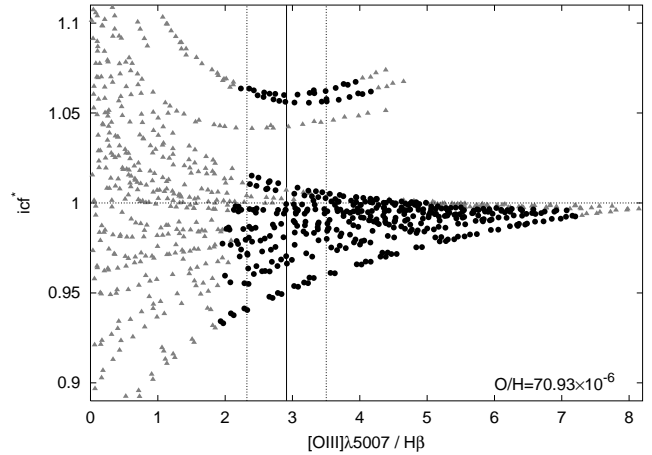


Fig. 11. Same as Fig. 10 but for models with high metallicity.

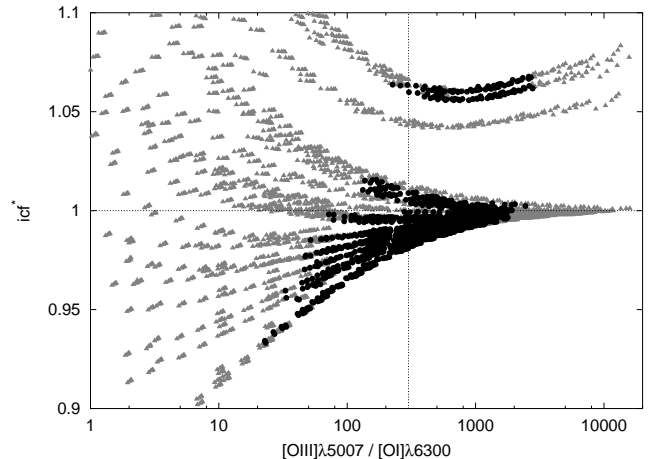


Fig. 12. Metallicity independent cutoff criterion by Ballantyne et al. (2000). This shows the icf^* versus the line ratio $[O III]\lambda 5007/[O I]\lambda 6300$. The cutoff value is marked by the dashed line.

variations in T_e arise because the thermal equilibrium depends strongly on the local abundance of different ionization stages of coolants as, for example, oxygen. In real nebulae temperature variations could be even more pronounced due to, for example, more complicated density structures, possibly inducing ‘real’ small-scale fluctuations in the temperature. Variations of T_e are typically only taken into account for the abundance estimate of metals, i.e. oxygen. This is accomplished by dividing the observed H II-region into two zones of different degree of ionization adopting different temperatures inferred from appropriate ions for each zone. The main problem in dealing with nebular temperatures is to find the appropriate mean temperature for the physical process considered. Since the line emissivities for different lines and ionization stages of different elements have varying temperature dependencies, the bulk of the emission of certain lines used for analysis

may originate from either within hotter or cooler regions than the helium line emission. This implies that, in order to obtain accurate results for each line, a different temperature, determined by a appropriate weighted average, would need to be employed (Peimbert 1967). This, however, is a far from straightforward task (cf. Peimbert et al. (2000)). Usually, the electron temperature influencing the emissivities of helium lines is assumed to be constant within the He^+ sphere. It is determined by observing the ratios between the flux of collisionally excited oxygen lines $[\text{O III}]\lambda\lambda 5007, 4959$ and $\lambda 4363$ (Aller 1984). Nevertheless, it is known that such lines are exponentially temperature sensitive and thus mostly originate within the hotter regions of the nebulae.

In order to quantify the potential uncertainty arising from this method of temperature determination, another correction factor tcf is introduced by

$$tcf = \frac{\alpha_{\text{He}}(\lambda, T_{[\text{O III}]}) \int n_e n_{\text{He}^+} dV}{\alpha_{\text{H}}(\text{H}\beta, T_{[\text{O III}]}) \int n_e n_{\text{H}^+} dV} \quad (11)$$

$$= \frac{\int n_e n_{\text{He}^+} \alpha_{\text{He}}(\lambda, T) dV}{\int n_e n_{\text{H}^+} \alpha_{\text{H}}(\text{H}\beta, T) dV}$$

$$= \frac{\int n_e n_{\text{He}^+} dV}{\int n_e n_{\text{H}^+} dV} \left/ \left(\frac{N_{\text{He}^+}}{N_{\text{H}^+}} \right)_{T_{[\text{O III}]}} \right.$$

where

$$\left(\frac{N_{\text{He}^+}}{N_{\text{H}^+}} \right)_{T_{[\text{O III}]}} = \frac{\alpha_{\text{H}}(T_{[\text{O III}]}) I(\text{He I}, \lambda)}{\alpha_{\text{He}}(T_{[\text{O III}]}) I(\text{H}\beta)} \quad (12)$$

Here $T_{[\text{O III}]}$ denotes the ‘‘average’’ temperature as derived from the oxygen lines. The tcf factor is unity for constant temperature within the whole emitting volume. For ‘‘normal’’ clouds this factor is smaller unity since the emission of $[\text{O III}]$ lines originates in regions with high amount of O^{2+} that do not coincide with the region where helium is ionized. Thus, this emission is weighted towards the hotter interior of the cloud. In contrast the main contribution to helium recombination lines is emitted within the outer, and thus cooler, parts of the cloud. Note, however, that in extreme cases the tcf may become larger than unity which is due to its implicit dependence on ionization structure (cf. Eq. 11). In such cases, nevertheless, the clouds are already characterized by extreme icf corrections.

Corrections due to temperature variations depend on the particular helium line considered since emissivities of different lines have different temperature dependencies. Observers sometimes employ the $\text{He I } \lambda 6678$ line alone because it is the line that is less suspect of enhancement due to collisional excitation than other He I lines. Other approaches use a weighted mean of all strong He I recombination lines. Of the commonly used He I recombination lines $\lambda 4471$, $\lambda 5876$, and $\lambda 6678$, the last should be most sensitive to potentially arising effects from temperature variations. Figure 13 shows the tcf versus η for all models computed in this work. It is derived as an equally weighted average of the tcf 's of the individual $\lambda 4471$, $\lambda 5876$, and $\lambda 6678$ lines. Because the metal lines provide the main cooling contribution, varying temperature effects are not only

a function of ionization structure but also depend strongly on metallicity. Thus, the tracks in Figure 13 are broader than those found for the icf^* corrections. From these calculation one may estimate a potential systematic overestimate of Y due to a non-ideal choice of temperature of up to 4%.

In case of strongly varying electron density, the effects of ionization structure and temperature variation are not anymore independent because higher order terms introduce a cross correlation between both effects. Since icf -effects, in some cases, may be considerably larger than tcf -effects this cross correlation may lead to unexpectedly high values for the ‘‘ideal’’ temperature yielding $tcf > 1$. Such models are characterized by extreme ionization structures. They certainly do not fulfill the simplified assumptions of distinct regions of high and low degree of ionization. Interestingly, however, even those regions show emission properties that may be observed in real clouds.

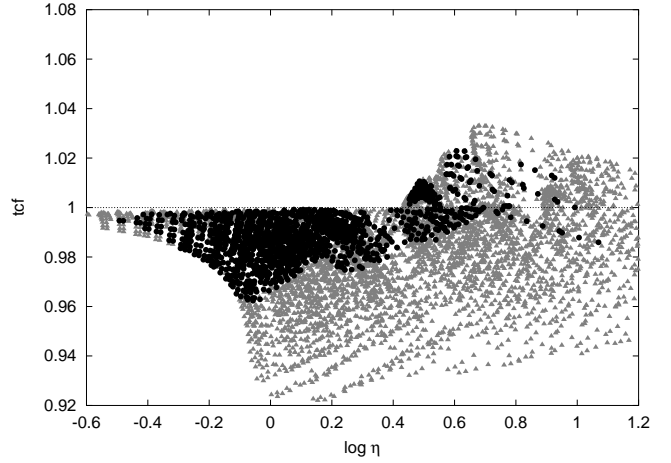


Fig. 13. Temperature correction factor tcf versus the Radiation Softness Parameter η for the whole sample of models computed.

In Fig.14 temperature correction factors are shown as a function of U_S and the quality of the incident continuum as given by the ratio $Q(\text{He}^0)/Q(\text{H}^0)$. The shown models have been computed with Mihalas spectra though results are very similar when different spectra are employed. It is evident that the tcf has its strongest dependence on U_S and is only mildly dependent on the spectrum. Those models which have tcf 's close to unity have large U_S and $Q(\text{He}^0)/Q(\text{H}^0) \gtrsim 0.15$ above the threshold for sufficient helium ionization. This is very similar to the behavior of icf -effects as discussed in the last section, such that both potential errors could be reduced if H II-regions of only very small radiation softness parameter $\log \eta < -0.5$ would be used for helium abundance determinations.

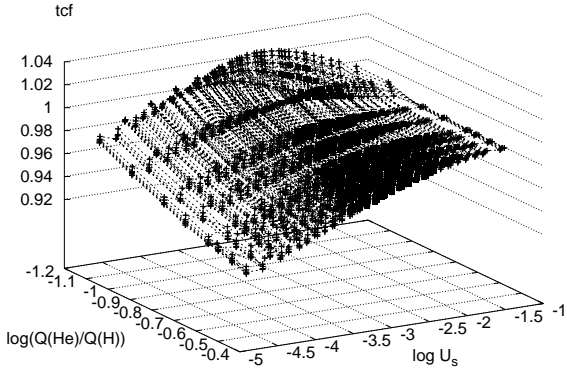


Fig. 14. tcf corrections versus the $Q(\text{He}^0)/Q(\text{H}^0)$ ratio and U_S for models ionized by Mihalas continua.

4. Discussion

From the results of the preceding section it is clear that potentially large uncertainties in the determination of helium abundances in low-metallicity H II-regions may arise due to the “imperfect” ionization structure of nebulae, as well as the existence of temperature variations. Moreover, both of the investigated systematic uncertainties point towards a potential overestimate of helium abundances, since observed H II-regions seem to be described by radiation softness parameters η which are indicative of possible “reverse” ionization corrections, rather than showing evidence for additional amounts of neutral helium. Fig. 15 shows the combined required correction factor, taking account of both effects, as a function of η . As before, models which fulfill the emission line range criteria are indicated by black symbols.

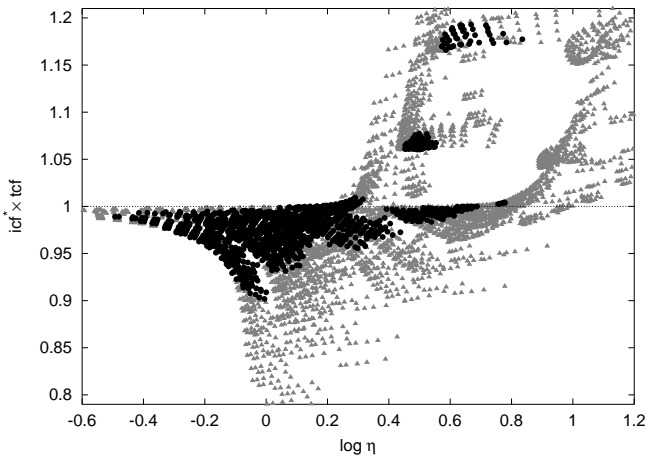


Fig. 15. The total required correction factor (icf^* and tcf) versus the Radiation Softness Parameter η for all models considered in this work.

Corrections for ionization structure seem to depend mostly on two parameters, the spectrum of the incident radiation, as well as the ratio of width to radius $\delta r_S/r_S$ of the Strömgen sphere. As long as the supply of helium ionizing photons is sufficient (i.e. $Q(\text{He}^0)/Q(\text{H}^0) \gtrsim 0.15$ corresponding to $\log \eta \lesssim 0.3$ within the assumed models) only “reverse” ionization corrections ($icf < 1$) occur. These ionization corrections could be, at least in principle, reduced to negligible levels when the ionization parameter at the Strömgen sphere becomes large, corresponding to small $\delta r_S/r_S$. This limit occurs for $\log \eta \lesssim -0.5$ for the model H II-regions employed here. Such corrections could also become small when matter-bounded nebulae are considered. In the intermediate regime $-0.5 \lesssim \log \eta \lesssim 0.3$ icf corrections may become appreciable with the required correction being larger for harder spectra. Non-uniform temperature corrections, parameterized by tcf , depend mostly on $\delta r_S/r_S$ with the dependence on spectrum of secondary importance. These corrections also have some dependence on metallicity, as it is known that low-metallicity clouds have shallower temperature gradients. Both corrections individually become most significant for radiation softness parameters $\log \eta \approx 0$ leading to the apparent “triangular” structure in Fig. 15.

Ionization correction factors in helium abundance determinations have been recently investigated by Armour et al. (1999); Viegas et al. (2000) and Ballantyne et al. (2000). The present work broadly confirms the potential problem of required “reverse” ionization corrections, though their are differences on the viability of proposed criteria to exclude such uncertainties as well as the magnitude of the uncertainties when variations in electron density is taken into account. Moreover, Ballantyne et al. (2000) infer an underestimate of the primordial helium abundance due to this effect, whereas Viegas et al. (2000) argue for only a moderate $\sim 1\%$ overestimate.

Steigman et al. (1997) concluded that the existence of temperature “fluctuations” in H II-regions leads to an underestimate of the primordial helium abundance. This underestimate is claimed to be the result of an underestimate of metal abundances, which leads to a decreased slope of helium abundance against metallicity, as well as to an overestimate of collisional enhancement of helium recombination lines. Whereas the present analysis has not studied the first effect, there is disagreement on the sign of the second effect. Steigman et al. (1997) lower the temperatures of H II-regions from the inferred $T_{[O III]}$ by a typical amount of $\Delta T \approx 2000$ K, in order to account for a systematic overestimate of temperature from collisionally excited oxygen lines. An overestimate of $\sim 20\%$ in temperature leads to an overestimate of $\sim 5\%$ in the helium abundances since the temperature dependence of the ratio of recombination emissivities α_H/α_{He} (cf. Eq. 12) is $\sim T^{0.25}$ for $\lambda 6678$, $\sim T^{0.23}$ for $\lambda 5876$, and $\sim T^{0.13}$ for $\lambda 4471$, respectively. Coincidentally, a value of $\sim 5\%$ is close to the largest tcf corrections found in this work. This correction may be compared to the potential error in derived collisional enhancement factors (taken from Kingdon &

Ferland (1995)) due to a possible overestimate of temperature. Most clouds in the sample of Izotov & Thuan (1998) have $n_e < 100 \text{ cm}^{-3}$. Assuming $n_e = 100 \text{ cm}^{-3}$ this change is $\sim 0.3\%$ for $T_{[\text{O III}]} \approx 10^4 \text{ K}$ and $\sim 1\%$ for $T_{[\text{O III}]} \approx 2 \times 10^4 \text{ K}$. Only for clouds of fairly large density $n_e \approx 300 \text{ cm}^{-3}$ and temperature $T_{[\text{O III}]} \approx 2 \times 10^4 \text{ K}$ does the “collisional error” become comparable $\sim 2.5\%$ to the error induced by employing the wrong temperature in the recombination coefficients. It is concluded that an overestimate of temperature leads in most cases to an overestimate of helium abundance.

Though the employed model H II-regions in this paper are probably still too simplistic to account for the structure of real H II-regions, it would be interesting to establish or refute whether existing observational data is consistent with systematic uncertainties of sign and magnitude as found in the previous section. In Fig. 17 helium abundances of the sample by Izotov & Thuan (1998) are shown as a function of the radiation softness parameter as inferred by these authors. It is striking to observe that H II-regions with $\log \eta \gtrsim 0$ do populate the area of lower helium $Y \sim 0.24$ abundance, whereas their lower η counterparts seem not to. The approximate transition region of this trend at $\log \eta \approx 0$ coincides with the peak of the triangular structure observed in Fig. 15, where the potentially largest correction factors were found. Note that the helium abundances shown in Fig. 15 are not corrected for stellar enrichment. One may wonder if the apparent correlation in this graph is caused by a correlation of the inferred η of H II-regions with cloud metallicity. In Fig. 16 radiation softness parameter is shown as a function of metallicity, illustrating that such a correlation does not exist. An explanation of the observed trend in Fig. 17 due to the existence of composite clouds, with one cloud illuminated by a hard spectrum ($icf \approx 1$) and another by a soft spectrum ($icf > 1$), seems also unlikely, since composite clouds should rarely have $\log \eta \lesssim 0.4$ (Viegas et al. 2000).

Though it is not clear how statistically significant the excess of low Y H II-regions for $\log \eta \gtrsim 0$ is, these findings seem suggestive that the investigated systematic uncertainties may indeed exist in the observational data. One may verify upon inspection of Figures 6, 8, and 14 that a sample of clouds illuminated by the same hard spectra, but with varying U_S (i.e. $\delta r_S/r_S$), may not explain such a trend. Nevertheless, the same figures (and the knowledge that lower branches in Figure 6 correspond to larger $Q(\text{He}^0)/Q(\text{H}^0)$, i.e. harder spectra) illustrate that a sample of clouds with typical $\log U_S \sim -3$ illuminated by spectra of varying hardness may easily explain the observed trend. This is illustrated in Fig. 18 where the combined correction factors are shown for a sample of models illuminated by Mihalas (1972) and starburst spectra, and for two particular values of U_S . If this indeed would be the explanation, helium abundances could be overestimated by a typical $\sim 4\%$, with required corrections in individual cases possibly as large as $\sim 8\%$.

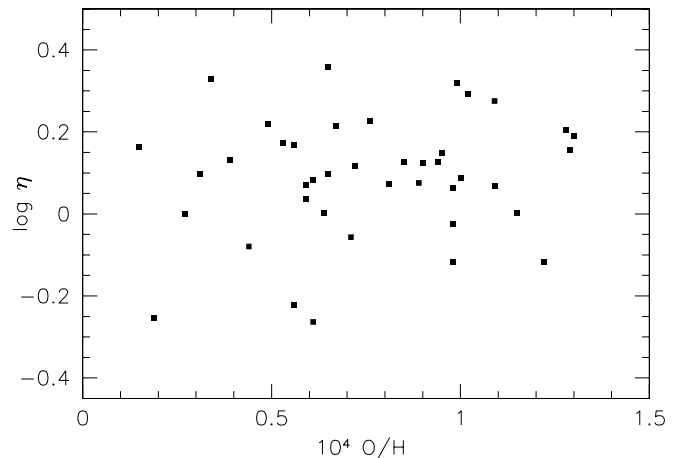


Fig. 16. Distribution of Radiation Softness Parameter η versus metallicity in terms of the oxygen to hydrogen ratio for the sample by Izotov & Thuan (1998).

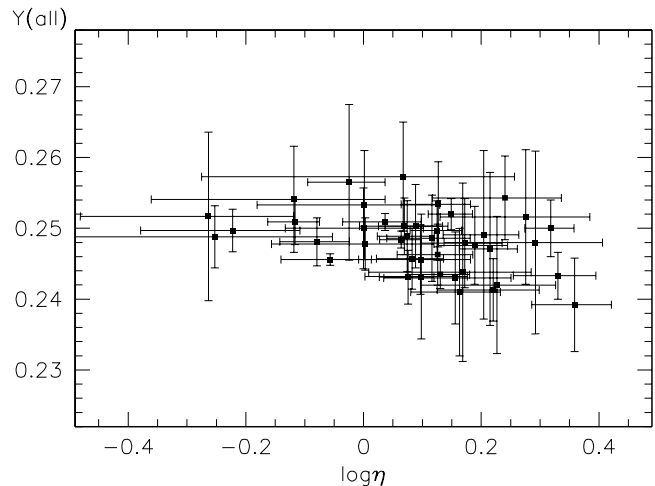


Fig. 17. Inferred helium mass fraction versus the Radiation Softness Parameter η for the sample of compact blue galaxies observed by Izotov & Thuan (1998).

5. Conclusions

The primordial helium abundance is commonly inferred from observationally determined helium abundances within low-metallicity extragalactic H II-regions. Such observational determinations may be subject to systematic uncertainties due to required corrections for existence of neutral hydrogen or helium (*icf*-corrections) and due to the possibility of non-uniform cloud temperature (referred to as *tcf*-corrections). These effects have been investigated in this paper. A chain of correction factors has been constructed that leads from the directly observable fluxes of helium- and hydrogen- recombination lines, and

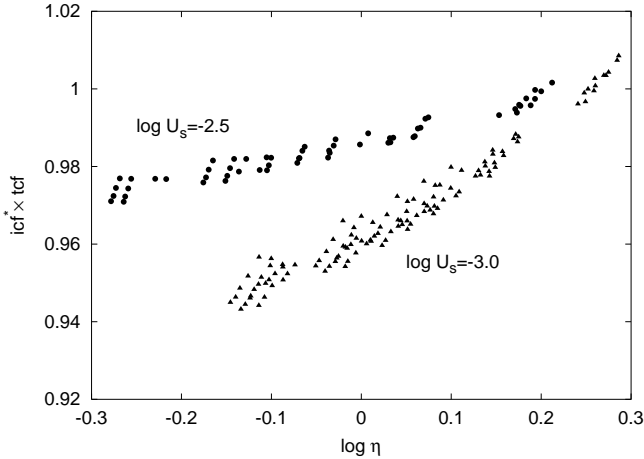


Fig. 18. Resulting total correction $tcf \times icf^*$ as a function of $\log \eta$ for models with (approximately) fixed U_S , as labeled. Shown are models illuminated by starburst and Mihalas spectra. All models fulfill the range criteria.

the inferred temperature from collisionally excited oxygen lines, to the true He/H ratio (cf. Eq. 12) in a nebula:

$$\frac{N_{\text{He}}}{N_{\text{H}}} = icf^* \times tcf \times \left(\frac{N_{\text{He}^+}}{N_{\text{H}^+}} \right)_{T_{[\text{O III}]}} \quad (13)$$

A large number of spherically symmetric model H II-regions with varying parameters and illuminated by ionizing radiation of different spectra have been constructed with the help of a photoionization code. It was shown that such models may be generally characterized by three physical quantities: the number of helium- to hydrogen- ionizing photons $Q(\text{He}^0)/Q(\text{H}^0)$, metallicity, and the ionization parameter at the Strömgren sphere U_S . It was also shown that U_S^{-1} is proportional to the ratio of width to radius $\delta r_S/r_S$ of the Strömgren sphere. The computed models are compared to the emission characteristics of observed H II-regions. A critical value for $Q(\text{He}^0)/Q(\text{H}^0) \gtrsim 0.15$ has been identified, such that for spectra above this critical value only reverse icf corrections apply. Such spectra result in clouds with radiation softness parameter $\log \eta \lesssim 0.3$. Reverse icf corrections may lead to a potentially large (up to $\sim 6\%$) overestimate of helium abundances, particularly for H II-regions of small $\log U_S$. These uncertainties may not easily be excluded even when $[\text{O III}]\lambda 5007/[\text{O I}]\lambda 6300$ -ratios (Ballantyne et al. 2000) are considered. In addition, a possible overestimate of helium abundances of similar magnitude (up to $\sim 4\%$) may be present due to the existence of temperature gradients, provided that temperature is inferred from collisionally excited oxygen lines. Both effects are absent only for H II-regions of extraordinarily small radiation softness parameter $\log \eta \lesssim -0.5$, corresponding to clouds of small $\delta r_S/r_S$ (large U_S) illuminated by sufficiently hard spectra. In contrast, the range of $-0.3 \lesssim \log \eta \lesssim 0.3$ is found for an existing sample of H II-regions (Izotov & Thuan 1998). Here required corrections may become large. This sample seems

to display a correlation between inferred helium abundance and radiation softness parameter in concordance with a typical overestimate of helium by about $\sim 2 - 4\%$. In case such an interpretation of the data should prevail, and when uncertainties leading to a possible underestimate of helium abundances due to other effects would be excluded, a downward revision of inferred primordial helium would be required.

Acknowledgements. The authors wish to acknowledge T. Abel and S. Burles for several helpful discussions and G. Ferland for communication.

References

- Aller, L. H. 1984, *Astrophysics and Space Science Library*, Vol. 112, *Physics of Thermal Gaseous Nebulae* (D. Reidel Publishing Company)
- Armour, M., Ballantyne, D. R., Ferland, G. J., Karr, J., & Martin, P. G. 1999, *PASP*, 111, 1251
- Ballantyne, D. R., Ferland, G. J., & Martin, P. G. 2000, *ApJ*, 536, 773
- Benjamin, R. A., Skillman, E. D., & Smits, D. P. 1999, *ApJ*, 514, 307
- Bresolin, F., Kennicutt Jr., R., & Garnett, D. 1999, *ApJ*, 510, 104
- Burles, S., Nollett, K. M., Truran, J. W., & Turner, M. S. 1999, *Physical Review Letters*, 82, 4176
- Dinerstein, H. L. & Shields, G. A. 1986, *ApJ*, 311, 45
- Ferland, G. J. 1997, *Hazy, A Brief Introduction to Cloudy 90*, University of Kentucky, Department of Physics and Astronomy Internal Report
- Ferland, G. J. 2000, private communication
- Grevesse, N. & Anders, E. 1989, in *AIP Conf. Proc.* 183: *Cosmic Abundances of Matter*, 1–8
- Izotov, Y. I. & Thuan, T. X. 1998, *ApJ*, 500, 188
- Izotov, Y. I., Thuan, T. X., & Lipovetsky, V. A. 1994, *ApJ*, 435, 647
- . 1997, *ApJS*, 108, 1
- Kingdon, J. B. & Ferland, G. J. 1995, *ApJ*, 442, 714
- Kunth, D. & Sargent, W. L. W. 1983, *ApJ*, 273, 81
- Kurucz, R. L. 1991, in *Proceedings of the Workshop on Precision Photometry: Astrophysics of the Galaxy*, ed. A. Davis Philip, A. R. Uppgren, & K. A. James, 27
- Kurucz, R. L. 1992, in *IAU Symp.* 149: *The Stellar Populations of Galaxies*, Vol. 149, 225
- Leitherer, C., Schaerer, D., Goldader, J. D., Delgado, R. M. G., Robert, C., Kune, D. F., de Mello, D. F., Devost, D., & Heckman, T. M. 1999, *ApJS*, 123, 3
- Mihalas, D. 1972, *Non-LTE Model Atmospheres for B & O Stars*, NCAR-TN/STR-76
- Olive, A. K. & Skillman, E. 2000, *astro-ph/0007081*
- Olive, K. A., Steigman, G., & Skillman, E. D. 1997, *ApJ*, 483, 788
- O’Meara, J., Tytler, D., Kirkman, D., Suzuki, N., Prochaska, J. X., & Wolfe, A. M. 2000, *astro-ph/0011179*
- Osterbrock, D. 1989, *Astrophysics of Gaseous Nebulae and Active Galactic Nuclei* (University Science Press)

- Osterbrock, D. & Flather, E. 1959, *ApJ*, 129, 26
- Pagel, B. E. J., Simonson, E. A., Terlevich, R. J., & Edmunds, M. G. 1992, *MNRAS*, 255, 325
- Pauldrach, A. W. A., Lennon, M., Hoffmann, T. L., Sellmaier, F., Kudritzki, R. ., & Puls, J. 1998, in *ASP Conf. Ser. 131: Properties of Hot Luminous Stars*, 258
- Peña, M. 1986, *PASP*, 98, 1061
- Peimbert, M. 1967, *ApJ*, 150, 825
- Peimbert, M., Peimbert, A., & Ruiz, M. . 2000, *ApJ*, 541, 688
- Peimbert, M. & Torres-Peimbert, S. 1974, *ApJ*, 193, 327
- Sasselov, D. & Goldwirth, D. 1995, *ApJ*, 444, L5
- Schaerer, D. & de Koter, A. 1997, *A&A*, 322, 598
- Schmutz, W., Leitherer, C., & Gruenwald, R. 1992, *PASP*, 104, 1164
- Skillman, E. D. 1989, *ApJ*, 347, 883
- Stasińska, G. 1980, *A&A*, 84, 320
- . 1990, *A&AS*, 83, 501
- Steigman, G., Viegas, S. M., & Gruenwald, R. 1997, *ApJ*, 490, 187
- Tytler, D., O’Meara, J. M., Suzuki, N., & Lubin, D. 2000, *Phys. ScrT*, 85, 12
- Viegas, S., Gruenwald, R., & Steigman, G. 2000, *ApJ*, 531, 813
- Vilchez, J. M. & Pagel, B. E. J. 1988, *MNRAS*, 231, 257